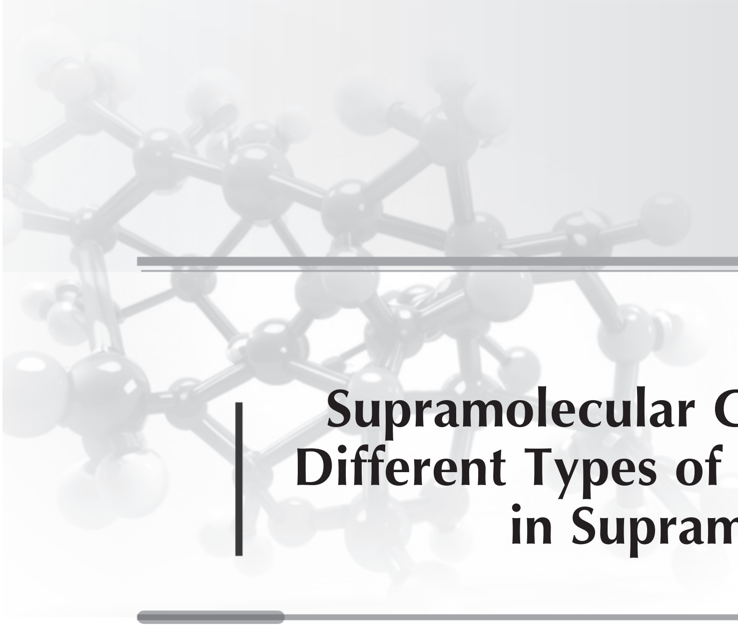

Chapter

1

Supramolecular Chemistry: Concepts and Different Types of Noncovalent Interactions in Supramolecular System

1.1 WHAT IS SUPRAMOLECULAR CHEMISTRY? (Refs. D.J. Cram, *Science*, **240**, 760, 1988, and *Angew. Chem. Int. Ed. Engl.*, **27**, 1009, 1988; J.M. Lehn, *ibid*, 27, 89, 1988)

The term 'supramolecular chemistry' means 'chemistry beyond the molecule'. In supramolecular systems, the molecular components (*i.e.* guests and hosts) are held together through the noncovalent intermolecular forces. Thus, it describes the chemistry of molecular assemblies held together through the noncovalent intermolecular forces. On the other hand, the molecular chemistry deals with the covalent bond formation.

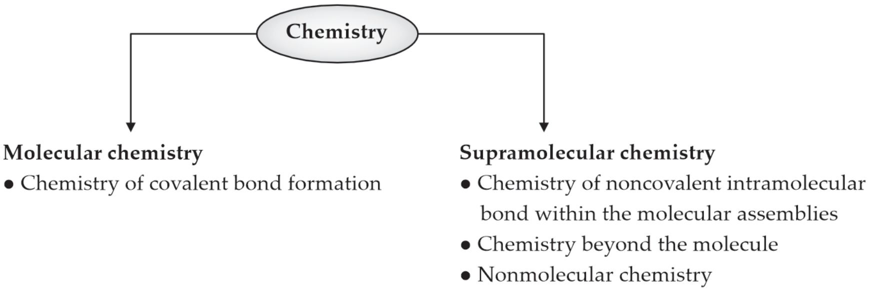

Molecular chemistry
- Chemistry of covalent bond formation

Supramolecular chemistry
- Chemistry of noncovalent intramolecular bond within the molecular assemblies
- Chemistry beyond the molecule
- Nonmolecular chemistry

In the **supramolecular assemblies** (also called the supermolecules), the components (*i.e.* guests and hosts) match both sterically and electronically so that the component molecules can recognise each other. This leads to **molecular recognition**. This is why, the chemistry of molecular recognition is also known as the **guest-host chemistry** (as introduced by DJ Cram in 1974). However, the popular term, supramolecular chemistry was introduced by JM Lehn in 1978.

- **Components and phenomena in molecular chemistry *vs.* supramolecular chemistry:**

Molecular chemistry	Supramolecular chemistry
Atom	Molecule
Covalent bond(s) between the atoms	Noncovalent intermolecular bonds
Synthon	Supramolecular synthon
Molecule	Molecular crystal
Covalent synthesis	Crystal engineering leading to the synthesis of molecular crystal

Transition state (for bond breaking/ formation)	Nucleus formation for crystallisation of molecules
Reaction	Crystallisation

Many of these aspects will be discussed later in detail (see Sec. 1.4).

Noble Prize in Chemistry, 1987, was jointly awarded to Donald J Cram, Jean-Marie Lehn and Charles J. Pederson for the development of **supramolecular chemistry**.

- **Supermolecules and supramolecular assemblies:** Generally, the large and complex molecules are described as the supermolecules and very often, the large complex biomolecules are called the supermolecules. In supramolecular chemistry, the supramolecular assemblies developed from the noncovalent intermolecular forces are also described as the **supermolecules**.

1.2 THE LOCK AND KEY PRINCIPLE IN SUPRAMOLECULAR ASSEMBLIES AND MOLECULAR RECOGNITION

In supramolecular systems, the attractive forces operate efficiently when the ***receptor*** (*i.e.* host) provides a suitable cavity or site that properly matches both *electronically* and *sterically* (*i.e.* properties related with the shape and size) with the *substrate* (*i.e.* guest). ***Thus, in the guest-host molecular assembly, the molecular components must maintain the proper complementarity both electronically and sterically***. This is why, the components of the supramolecular assembly can recognise each other through the interplay of supramolecular noncovalent forces. This leads to ***molecular recognition*** and the molecular recognition leads to the supramolecular assemblies which are also described as the **supermolecules**.

To recognise the substrate (*i.e.* guest), the receptor (*i.e.* host) must be suitably designed. This is illustrated in Fig. 1.2.1(a). For the molecular recognition, very often, different **macropolycyclic receptors** with the cavities of different shape and size are used (Fig. 1.2.1(b)).

***Guest* (G) + *Host* (H) $\rightleftharpoons$ Guest–Host (G–H) complex (supramolecular assembly)**

The stability of a supramolecular system (*i.e.* receptor-substrate assembly) depends on the degree of ***stereoelectronic fit*** among the components (*i.e.* molecular building blocks). Thus, in supramolecular systems, the ***lock and key principle*** (found in the enzymatic activity) is followed. Because of this principle, the selectivity of the enzyme is attained. The supramolecular interaction is important in many other biomolecules (*e.g.* proteins, DNA, etc.).

The lock and key principle representing the guest–host interactions is illustrated in the following examples.

Hosts:	Enzyme	Receptor	Receptor	Antibody	Ligand
Guests:	Substrate	Substrate	Drug	Antigen	Metal

In the last three decades, a vast amount of work has been carried out in understanding the supramolecular chemistry and in developing the different types of ***receptors for molecular recognition***. Knowledge of the supramolecular chemistry finds many applications. This field has been recognised by the award of a **Nobel Prize in 1987** to D.J. Cram, J.M. Lehn and CJ Pedersen.

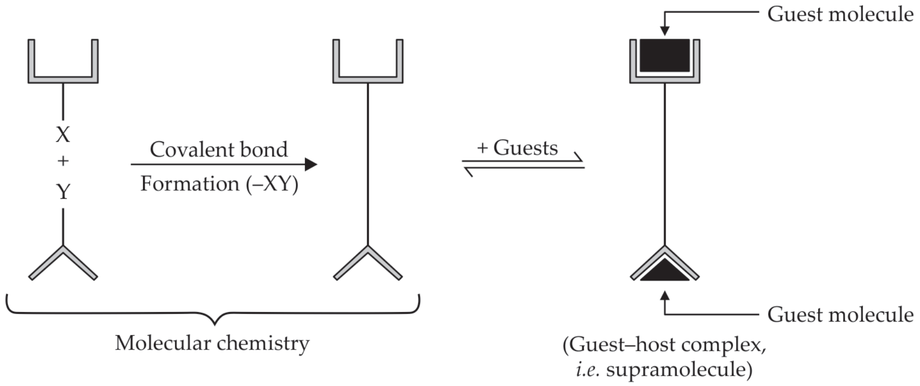

(a) Illustration of supramolecular chemistry

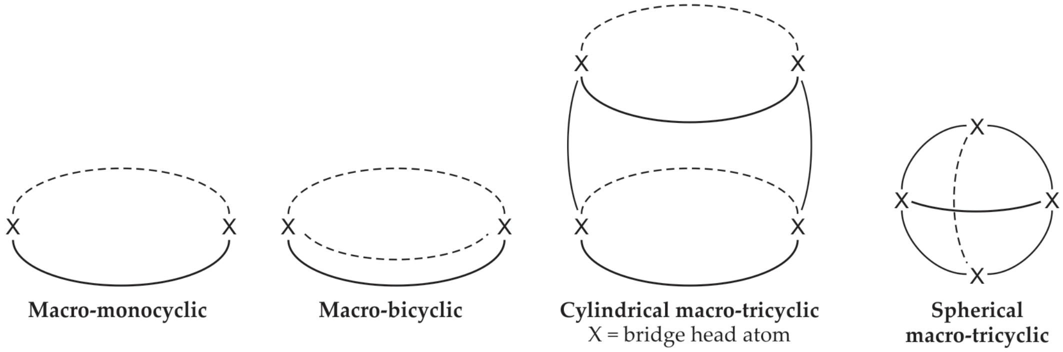

(b) Macrocyclic receptors

Fig. 1.2.1: Illustration of supramolecular chemistry and representation of different macrocyclic receptors (*i.e.* hosts) used in molecular recognition through the guest–host complex formation

1.2.1 Supramolecular Interactions (Based on the Lock and Key Principle) in Substrate Specificities of Enzymes

A typical enzyme-substrate selectivity example is illustrated in the enzyme catalysis by Zn(II) containing **carboxypeptidase-A** enzyme that selectively catalyses the **hydrolysis of C-terminal peptide** linkage. This enzyme shows a marked preference towards such peptide linkages in which the side chain of the terminal residue contains some aromatic moiety or branched aliphatic chain with L-configuration. **Arg-145 residue** participates in C-terminal peptide linkage recognition and the **chiral hydrophobic cavity** located at the vicinity of active site houses the hydrophobic group (θ) of the C-terminal residue of the substrate. Besides Arg-145, that is mainly responsible for substrate specificity, other amino acid residues like Arg-127 and Asn-144 also participate in substrate docking. This is illustrated in Fig. 1.2.1.1.

- **Carboxypeptidase-A *vs* carboxypeptidase-B:** Arg-145 residue acts as the **docking position** of C-terminal end of the peptide chain in both these **exopeptidase Zn(II)-containing enzymes**. In carboxypeptidase-A (CPA), the **chiral hydrophobic pocket** gives **enantioselectivity**. This hydrophobic cavity can **accommodate the side chain of L-phenylalanine but not that of D-phenylalanine**. In general, this hydrophobic pocket

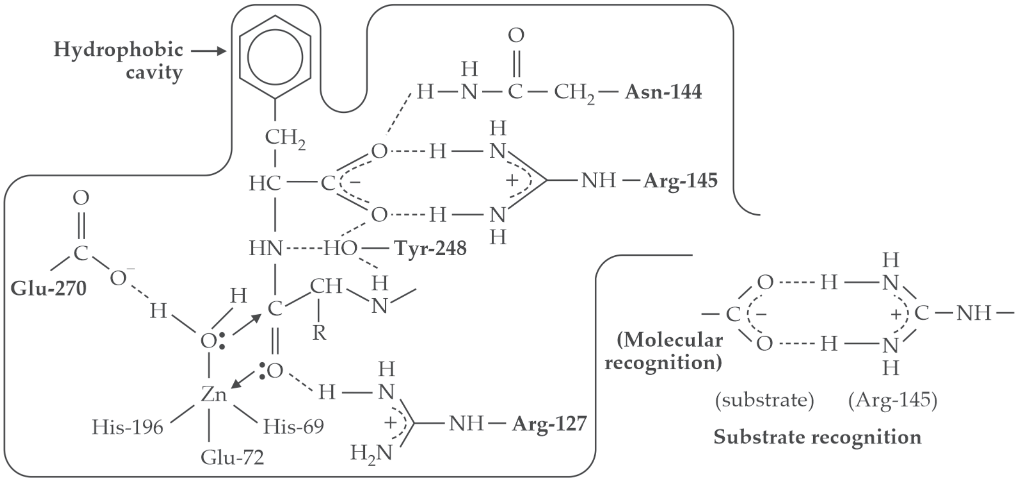

Fig. 1.2.1.1: Schematic illustration of noncovalent supramolecular interactions of substrate binding (*i.e.* the molecular recognition) at the active site of carboxypeptidase-A

Note: Arg for arginine, **His** for histidine, **Asn** for asparagine, **Asp** for aspartic acid, **Glu** for glutamic acid, **Tyr** for tyrosine, **Ser** for serine. The amino acid sequence of a polypeptide chain is written in the direction, N-terminal end →C-terminal end.

The amino acid sequence in a polypeptide chain is denoted by number. For example, **Arg-145** indicates that this amino acid is at the 145 position counted from the N-terminal end of the peptide chain.

can accommodate the aromatic or aliphatic hydrophobic moiety of the side chain of C-terminal amino acid residue and this is why, CPA is highly specific for the C-terminal peptide bond where the C-terminal residue is bearing the **aromatic or aliphatic hydrophobic moiety** as in phenylalanine or leucine. This preference justifies the name CPA, where **A stands for aromatic/aliphatic**.

In the case of carboxypeptidase-B (CPB), the corresponding **anionic pocket** generated by Asp-255 accommodates the **cationic basic side chain** of the C-terminal amino acid. Thus CPB preferably hydrolyses the C-terminal peptide bond where the C-terminal residue bears a basic side chain (*e.g.* lysine, arginine) that remains protonated at the biological pH to **provide the cationic side chain**. It justifies the name CPB, where **B stands for the basic side chain**. These are illustrated in Fig. 1.2.1.2.

- **Substrate specificity of chymotrypsin *vs* trypsin:** It is illustrated in Fig. 1.2.1.3.

1.3 SUPRAMOLECULAR INTERACTIONS: DIFFERENT TYPES OF NONCOVALENT INTERMOLECULAR INTERACTIONS

1.3.1 The Important Types of Supramolecular Interactions

The important supramolecular forces which are noncovalent in nature are:

- Electrostatic interactions (*e.g.* ion–ion, ion–dipole, dipole–dipole, etc.)
- van der Waals interactions including London dispersion forces.
- Hydrophobic (*i.e.* solvatophobic) effect (basically an **entropy driven effect**).
- Hydrogen bonding.
- Halogen bonding.

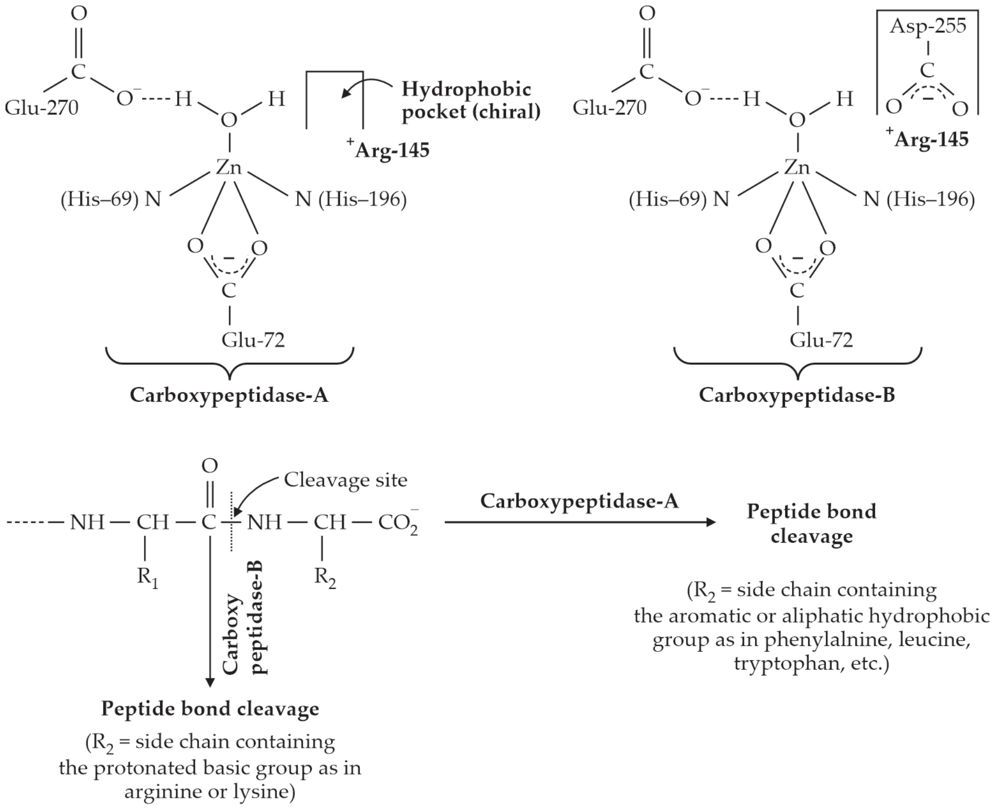

Fig. 1.2.1.2: Comparison of the active sites of carboxypeptidase-A and -B enzymes and their substrate specificities

- Aromatic interactions (*e.g.* π–π stacking interaction, cation-π interaction, anion-π interaction).
- Closed shell interaction — strengthened by relativistic effect (*e.g.* **aurophilicity**, secondary bonding, halogen bonding by the heavier halogens, etc.)
- **Metal-ligand coordination** treated as ion-dipole or ion-ion electrostatic interaction.

However, in metal–ligand coordination, involving the transition metal ions, the *metal–ligand interaction is not surely a pure noncovalent interaction.*

Note: ● The **strong bonds** (bond energy, 100–1000 kJ mol^{-1}) like covalent, ionic and metallic bonds are called the **primary bonds** while the **weak noncovalent bonds** (bond energy, 1–50 kJ mol^{-1}) like H-bonds and van der Waals bonds are described as the **secondary bonds**, leading to **supramolecular assemblies**.

● **Hydrogen bonding** (specially the **directional strong H-bonding**), **halogen bonding, aurophilic interaction, metal-ligand interaction**, etc. are not surely the examples of strict noncovalent interactions. However, such interactions are widely considered as the supramolecular interactions because these interactions very often lead to the development of supramolecular architectures.

All the intermolecular weak forces, *i.e.* **secondary bonds**, including the van der Waals interactions, dispersion interaction, electrostatic interaction, and H-bonding interaction have been discussed in detail in Chapter 13, Vol. 3, **Fundamental Concepts of Inorganic Chemistry**, Vol. 2.

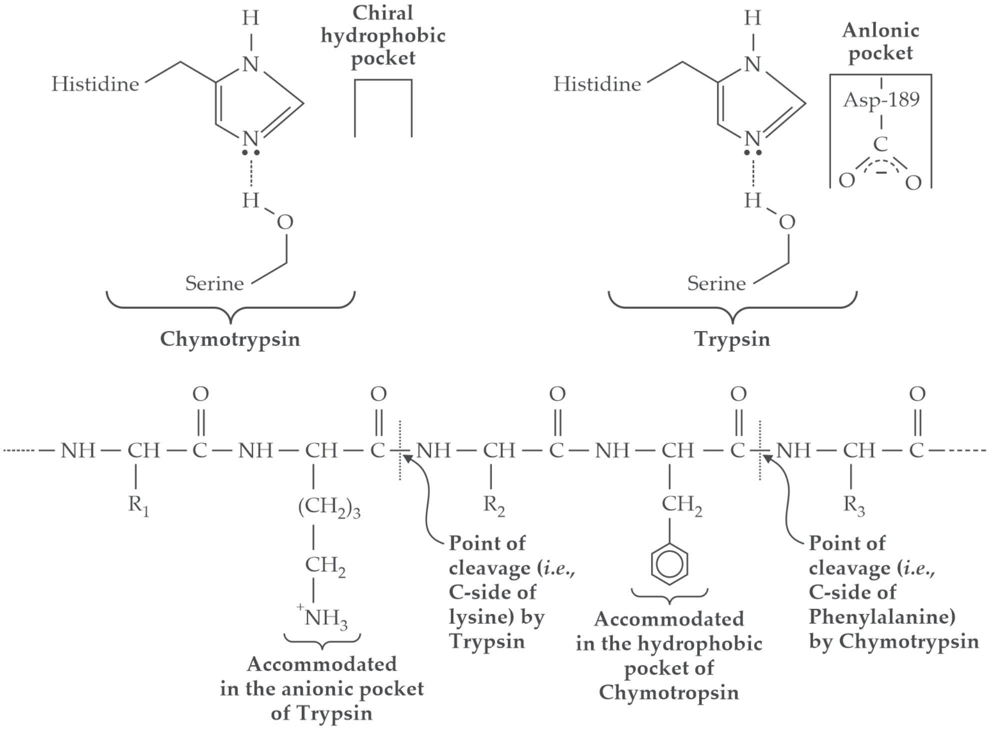

Fig. 1.2.1.3: A comparison of the active sites of the endopeptidases - chymotrypsin and trypsin to determine their substrate specificities

Note 1: Chymotrypsin and trypsin are not the metalloenzymes. They are the **serine peptidases** where a serine residue (Ser—OH) makes the nucleophilic attack on the peptide linkage as the serinate or alkoxide (Ser–O⁻) through the proton transfer from the serine residue to a histidine residue.

$$\text{Ser}-\text{O}\diagdown\text{H}---\text{Im}-\text{His}\longrightarrow\text{Ser}-\overset{-}{\text{O}}---\overset{+}{\text{H}}\text{im}-\text{His}$$

Chymotrypsin and carboxypeptidase-A are associated with the similar type **hydrophobic pocket** at the active site. On the other hand, trypsin and carboxypeptidase-B possess the similar type **anionic pocket** at the active site.

Note 2: For details of the enzymatic activities of different enzymes, the readers may consult the authors' book, *Biophysical, Bioorganic and Bioinorganic Chemistry*.

In this Section, we shall discuss the origin of **halogen bonding** and **hydrophobic effect** in detail and recapitulate the other intermolecular forces. Table 1.3.1.1 compares the interaction energy of different types of intermolecular forces and their dependence on the **interacting distance** (r).

1.3.2 Ion-Ion Electrostatic Interactions

The electrostatic interaction between the oppositely charged ionic moieties is controlled by **Coulomb's law**. The electrostatic interaction energy (in CGS system) is given by:

$$E = \frac{q_1 q_2}{Dr}$$

Table 1.3.1.1: Comparison of different types of supramolecular interactions

Interaction	*Energy dependence on distance (r)*	*Typical energy (kJ mol^{-1})*	*Examples*
i. **Ion–ion**	$1/r$	~500	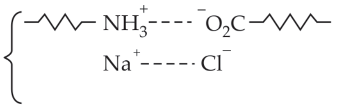
ii. **Ion-dipole**	$1/r^2$	~30–200	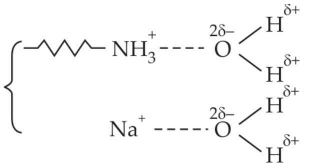
iii. **Dipole–dipole**	$1/r^3$ (stationary dipoles) $1/r^6$ (rotating dipoles, thermal effect)	–5 –1.5	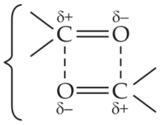
iv. **Ion-induced dipole**	$1/r^4$	~10	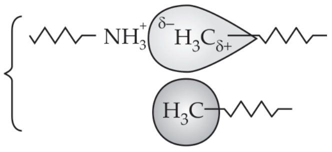 (*cf.* Me group without any polarization)
v. **Dipole-induced dipole**	$1/r^6$	–0.3	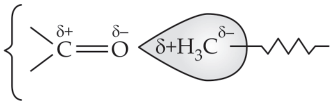
vi. **Dispersion** (London interaction)	$1/r^6$	~2.0	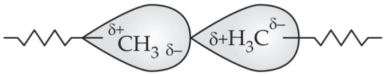
vii. **Hydrophobic bond**	–	~4.0	
viii. **Hydrogen bond**	–	20–40 (see Table 1.3.7.1)	X—H····A (X, A = N, O, F)
ix. **Cation-π**	–	~10–80	K^+····C_6H_6
x. π–π	–	~2–30	Graphite, benzene crystal

q_1 and q_2 = charges of the interacting moieties; D = dielectric constant of the medium; r = distance between the interacting centres.

Here it is evident that the value of dielectric constant (D) is playing a crucial role. It is the characteristic feature of the medium (*cf.* $D = 1$ in air; $= 80$ in water; $= 2–4$ in a nonpolar hydrophobic medium). Thus, the electrostatic attractive force in the nonpolar hydrophobic media is higher than that in water (Fig. 1.3.2.1).

1.3.3 Ion–Dipole Interactions

It basically represents the electrostatic interaction. The negative ends of the dipoles are oriented towards the cations while the positive ends of the dipoles are projected towards the anions. The cation and anion hydration are the representative examples $(Na(OH_2)_x^+$,

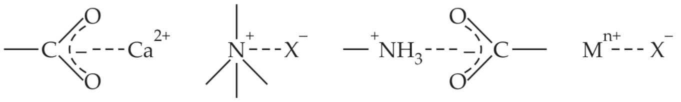

Fig. 1.3.2.1: Some representative ion–ion attractive interactions.

Note 1: Anions interacting with the metal centres may lead to the coordination compounds like $[FeF_6]^{3-}$, $[CoCl_4]^{2-}$, etc. but **these are not regarded as the supramolecules**.

Note 2: Electrostatic cation-anion interactions are the supramolecular interactions, but **ionic lattices like NaCl, KCl, etc. are not the examples of supramolecules**. These are regarded as the **ionic crystals.**

$Cl(H_2O)_y^-$, etc.). In fact, the metal ion–dipole interaction as in aquo, ammine, crown ether, etc. metal-complexes belongs to this class. This interaction energy depends on the alignment of the dipoles.

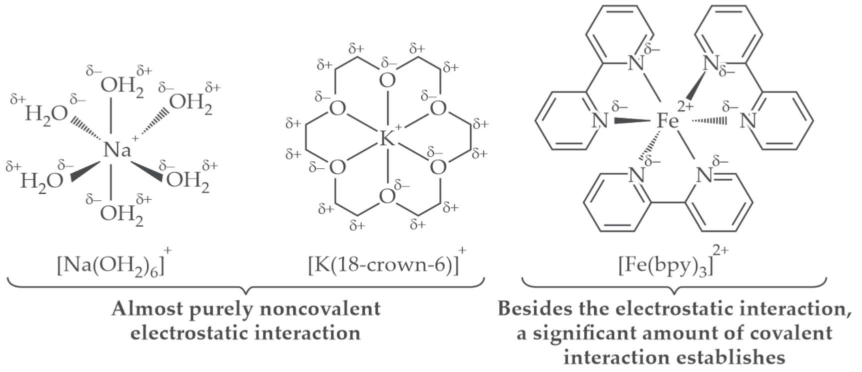

Fig. 1.3.3.1: Some representative examples of ion–dipole interaction in coordination complexes

Note: Metal–ligand interaction in the coordination compounds like $[Co(NH_3)_6]^{3+}$, $[Fe(bpy)_3]^{2+}$, etc. — is it purely a noncovalent electrostatic interaction? No, in the transition metal complexes, there is a good deal of covalent interaction. This is why, such **coordination compounds are not the examples of supramolecules**.

1.3.4 Dipole–Dipole Interaction (Keesom Forces)

The dipoles with their opposite ends tend to be oriented for the better electrostatic interaction but thermal agitation may tend to randomise their orientations (Fig. 1.3.4.1).

1.3.5 Dipole–Induced–Dipole Interaction: Distortion Effect (Debye Forces)

The electrical field of a permanent dipole can induce a dipole moment in an adjacent molecule (which may be polar or nonpolar). Thus the induced dipole can electrostatically interact with the inducing or polarising dipole. Obviously, the Debye force appears quite important when a permanent dipole interacts with a nonpolar molecule (*i.e.* when the Keesom force is absent). In such cases, the interaction energy is favoured more for the higher dipole moment of the polarising permanent dipole (say H_2O) and the higher **polarisability** of the nonpolar molecule (say inert gas Kr). The larger molecules, in general, are more polarisable. The stability of noble gas hydrates largely depends on the Debye forces because in these gas hydrates, the Keesom force is absent (Fig. 1.3.5.1).

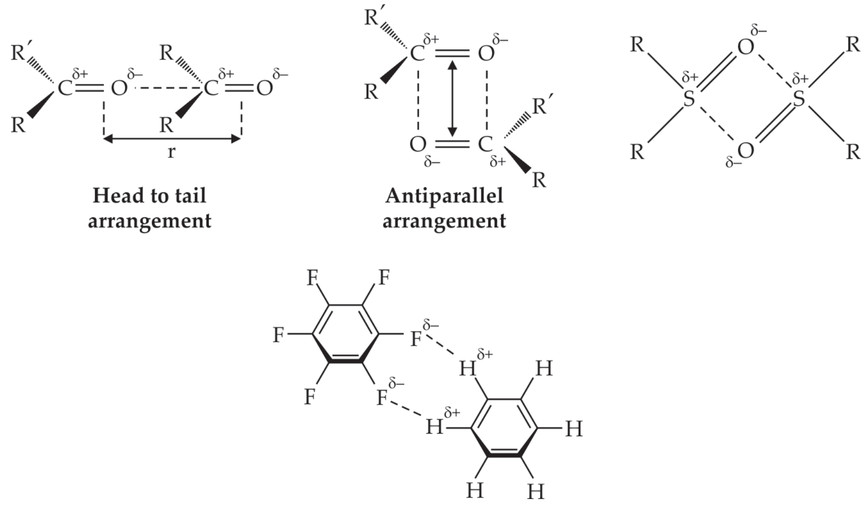

Head to tail arrangement

Antiparallel arrangement

Fig. 1.3.4.1: Some representative examples of dipole–dipole interaction

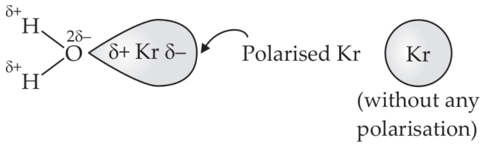

(without any polarisation)

Fig. 1.3.5.1: Illustration of dipole–induced–dipole interaction between H_2O and nonpolar Kr

1.3.6 Instantaneous Dipole-Induced-Dipole Interaction (London Dispersion Force)

Because of the fluctuations in the instantaneous positions of the electrons, a nonpolar molecule also possesses an instantaneous/transient dipole moment which can induce an instantaneous dipole moment in the nearby nonpolar molecule to interact electrostatically. This electrostatic interaction between the two instantaneous dipoles is called the **London dispersion force** which depends on the **polarisability of the interacting molecules**. The polarisability generally increases with the increase of molecular size. It explains the order of intermolecular attractive forces among the nonpolar halogen molecules (Fig. 1.3.6.1).

$$I_2 \text{ (solid)} > Br_2 \text{ (liquid)} > Cl_2 \text{ (gas)} > F_2 \text{ (gas)}$$

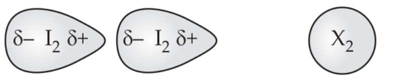

Halogen molecule without any polarisation

Fig. 1.3.6.1: Illustration of London dispersion force interacting between two instantaneous dipoles of two I_2 molecules

Note: London dispersive force is an **attractive** intermolecular/interatomic force. **Thus the term 'dispersive force' is misnomer.**

- **Dispersive forces: London force *vs* Casimeir-Polder (CP) force:** Dispersive forces (electromagnetic forces) occur between the molecules/atoms possessing no permanent electric dipole moment due to **quantum fluctuations of molecular or atomic electric dipole moments**. Thus, the dispersion forces are of **pure quantum origin**.

Dispersive forces are of two types: **nonretarded and retarded**. London dispersive forces (1930) **acting at very short distances** upto a few nanometers refer to nonretarded forces that appear considering the speed of light to be infinite. This assumption leads to the **instantaneous interaction**. CP forces (1948) act at larger separation distances where the retardation effect is taken into consideration. In the retarded interaction, **due to the finiteness of interaction propagation speed**, the dipole effect of a first molecule/atom will reach a second one after a time interval of r/c and the effect of second molecule/atom on the first one will be delayed by $2r/c$. These **delayed interactions decrease the correlation between the fluctuating electric dipoles.** This causes the retarded CP-forces to **drop more rapidly with distance than the nonretarded London forces**.

Obviously, the approximations (*i.e.* no delayed interaction) in the nonretarded London forces are valid where the separation distance between the interacting molecules/atoms is small (*i.e.* $r/c \rightarrow 0$).

In terms of origin (*i.e.* **quantum fluctuation of electric dipoles**), both the London and CP forces are of the same kind (*i.e.* dispersive forces). In the London force acting at very short distances, the retardation effect is neglected while in the CP forces acting at relatively larger distances, the retardation effect is taken into consideration. Obviously, there is some transition regions between these two kinds of dispersion forces. In fact, the **unified theory** of these two forces was developed by **Lifshitz in 1950**.

1.3.7 Hydrogen Bonding Interaction

It is a special type of dipole-dipole interaction. It is represented as: $\mathrm{X{-}H\cdots Y}$, where X and Y are the electronegative centres, X—H group is called the **H-bond donor** (denoted by D) while Y with the nonbonding lone pairs is called the **H-bond acceptor** (denoted by A). Considering the **charge separation** due to the bond polarisation, the H-bond segment $\mathrm{X^{\delta-}{-}H^{\delta+}\cdots Y^{\delta-}}$, *i.e.* $\mathrm{X^{\delta-}{-}H^{\delta+}\cdots A^{\delta-}}$ can be simply represented as: $\mathrm{A^{\delta-}\cdots D^{\delta+}}$ which is stabilised by an electrostatic interaction between the electropositive H-atom of the donor group (D) and electronegative centre of the acceptor group (A).

Note: In terms of the electron donation/acceptance, A is the **electron donor group** while the X—H segment is the **electron acceptor (A) group**. Thus, the **electron donor (D) group acts as the H-bond acceptor** and the **electron acceptor moiety acts as the H-bond donor**.

● **Classification of H-bonds in terms of H-bond strength:** Depending on the strength of H-bond, these can be classified into **three (A) groups:** *strong*, *moderate* and *weak*. The $\mathrm{C{-}H\cdots N/O}$, $\mathrm{O{-}H\cdots\pi}$, $\mathrm{C{-}H\cdots\pi}$, etc. are the **typically weak H-bonds**. There is no sharp line of distinction among these three types of H-bonds. With the increase of strength, the bond angle $\mathrm{X{-}\widehat{H}\cdots Y}$ tends towards 180° and the bond becomes more symmetrical (*i.e.* position of 'H' becomes almost equidistant from X and Y). The characteristic properties of these three types of H-bonds are shown in Table 1.3.7.1.

Convention to Represent a H-Bond

IUPAC (2011) recommended (*Ref. Pure. Appl. Chem.*, **83**, 1637 (2011), a **three dotted line** (···) to represent the H-bond (*e.g.* $\mathrm{X{-}H\cdots Y}$) but it is not strictly followed in the literature including the present book. **Dotted lines** (but not necessarily three dots) and **broken lines** are used to represent the H-bond (*cf.* solid line to represent the conventional covalent bond).

Table 1.3.7.1: Comparison of the properties of different types of H-bonds (X—H···A) (*cf.* covalent bond energy: 220–450 kJ mol^{-1})

	Weak	*Moderate*	*Strong*
Bond energy (kJ mol^{-1}):	2–20	20–60	60–120
X—H···A angle:	90–150°	120–170°	~180°
A···H distance:	220–320 pm	150–220 pm	120–150 pm
X···A distance:	320–400 pm	250–320 pm	220–250 pm
Bond character:	Electrostatic	Mainly electrostatic	Covalent (3*c*–4*e*)
Examples:	C—H···A, where A = F, N, O; C—H···π; O—H···π bifurcated and trifurcated H-bonds	Acids, Amides, Alcohols, Biomolecules like DNA, protein, etc.	Acid-dimers (gas phase), HF_2^-, H_3O^+, $H_5O_2^+$, $H_9O_4^+$, proton sponge

H-Bonding — is it purely a noncovalent electrostatic interaction?

The strong H-bonds maintain the **directionality** (*i.e.* X—H···Y linear) and this can be best explained by the **3*c*–4*e* covalent bonding** involving the main contribution of the donation of the nonbonding electron pair of Y into the vacant $\sigma^*_{X—H}$MO, *i.e.* NBMO(Y) → σ*(X—H) (*cf.* Fig. 1.3.8.1). For details of the 3*c*–4*e* H-bonding, please see Chapter 11, Vol. 2 of Fundamental Concepts of Inorganic Chemistry.

- Geometries of H-bonds: There are various types of geometries of H-bonds and these are shown in Fig. 1.3.7.1.

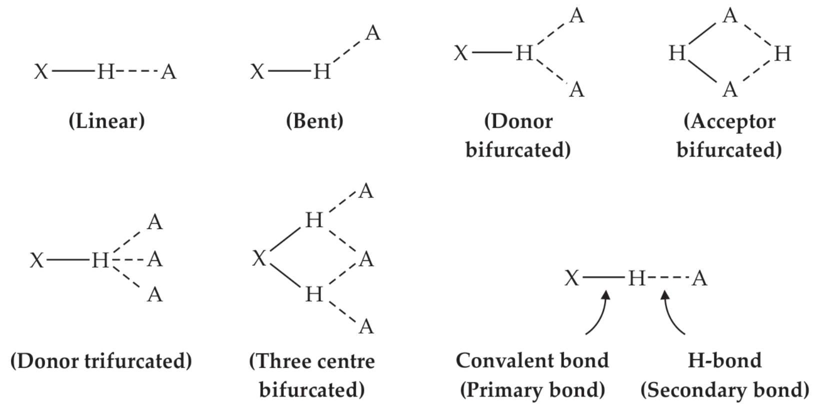

Fig. 1.3.7.1: Illustration of different types of geometries of H-bond.

Examples of Some Strong H-bonds

- A typical **single covalent bond energy:** 230–450 kJ mol^{-1}.
- **Symmetric *vs* asymmetric H-bonds:** In a strong H-bond as in HF_2^- or proton sponge, the X···H and H···A distances are almost equal provided X = A (denoted by X···H···A). Such H-bonds are called the **symmetric H-bonding**. The weak H-bonds are **asymmetric,** *i.e.* the X···H distance is shorter than the H···A distance (denoted by X—H···A). In a symmetric H-bonding, proton transport (see Fig. 12.4.1) is very fast (**Grotthuss mechanism**).

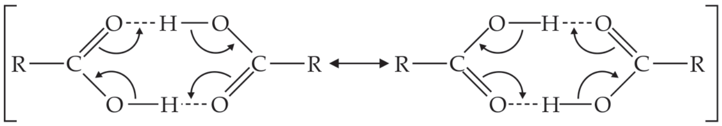

Acid dimers (gas phase)

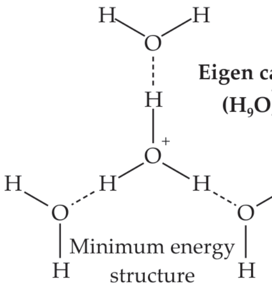

Eigen cation $(H_9O_4^+)$

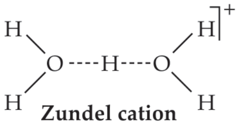

Zundel cation $(H_5O_2^+)$

$$\left[F\text{----}H\text{----}F\right]^-$$

(HF_2^-)

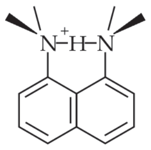

Proton sponge

- **Chemical shift (PMR signal):** Downfield shift with the increase of H-bond strength.
- **IR-Shift (X—H bond):** Due to n(**A**) → **σ*(X—H)** donation, *i.e.* donation of the nonbonding electron pair of NBMO of A into the vacant σ*-MO of the X—H bond, **red-shift** is noted. In some special cases, where the said donation is inefficient and the **X—H bond polarisation** through the increase of *s*-character in the hybrid orbital of X is the predominant factor (*cf.* **Bent's Rule**), **blue-shift** is noted. Such H-bonds are called the **improper H-bonding** (*JACS*, **125**, 5973, 2003) and noted when the **C—H bonds act as the H-bond donor groups.**
- **X—H···π interaction:** The filled π-BMOs (*i.e.* HOMOs) of the unsaturated organic compounds act as the electron donor orbital. Thus, it involves the $\pi_{HOMO}(A) \rightarrow \sigma^*(X—H)$ donation.
- **Diagonal secondary electrostatic interactions in the arrays of H-bonds:** It has been already pointed but that a H-bond (*i.e.* $X^{\delta-}—H^{\delta+}\cdots A^{\delta-}$ represented simply by $D^{\delta+}\cdots A^{\delta-}$) is stabilised due to the electrostatic attractive interaction. In a system of arrays of H-bonds between the complementary sites of hosts and guests, there are **two types** of electrostatic interactions: **primary electrostatic interaction** representing the **direct** electrostatic attractive interaction between the H-bond donor ($D^{\delta+}$) and acceptor ($A^{\delta-}$) groups; the **diagonal secondary** electrostatic **interactions** (which may be **attractive or repulsive** depending on the conditions) between the adjacent H-bonds (*i.e.* $D^{\delta+}\cdots A^{\delta-}$) playing a crucial role to determine the overall stability of an array of H-bonds as proposed by Jorgensen (*cf. JACS*, **112**, 2008, 1990).

The diagonal secondary electrostatic interactions in the arrays of H-bonding systems are illustrated in Fig. 1.3.7.2. It has been estimated that the **said diagonal secondary electrostatic interactions contribute approximately 30% of the primary electrostatic interactions.**

1.3.8 Halogen Bonding: An Important Noncovalent Interaction in the Formation of Supramolecular Architecture

Halogen bonding is quite analogous to the well known hydrogen bonding. In halogen bonding, halogen acts the electron acceptor while in hydrogen bonding, electron deficient hydrogen acts as the electron acceptor.

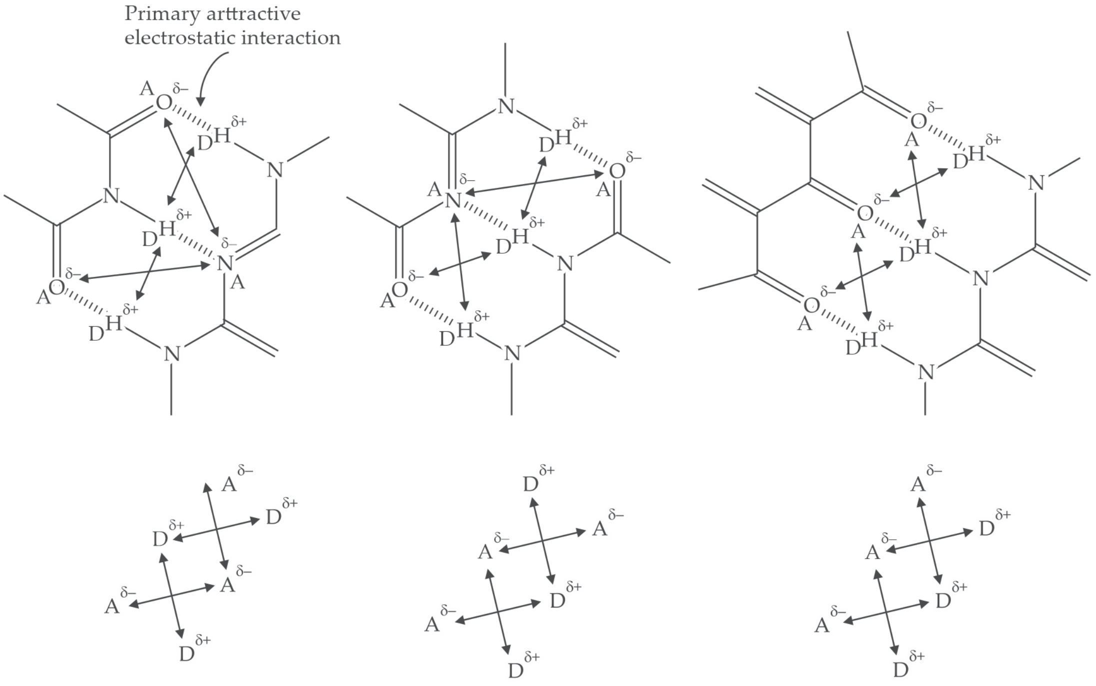

ADA-DAD
(AII diagonal secondary
electrostatic interactions
repulsive)

DAA-ADD
(Diagonal secondary
electrostatic interactions
2 repulsive, 2 attractive)

AAA-DDD
(All diagonal secondary
electrostatic interactions
attractive)

Stability order: DDD — AAA > DAA — ADD > ADA — DAD

Stability of the system: ADA — DAD ⟶ DAA — ADD ⟶ DDD — AAA

Increasing trend

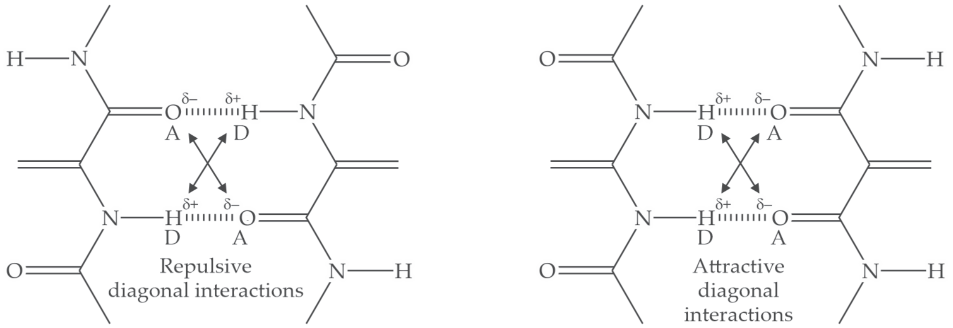

AD-DA system
Stability: ~50 kJ mol^{-1}

DD-AA system
Stability: ~98 kJ mol^{-1}

(**D** stands fot the **H-bond donor** and **A** stands for the **H-bond acceptor**)

Fig. 1.3.7.2: Illustration of the effect of diagonal secondary electrostatic interaction on the stability of the arrays of H-bonding (primary attractive electrostatic interaction denoted by ||||||||; diagonal secondary electrostatic interaction denoted by ↔).

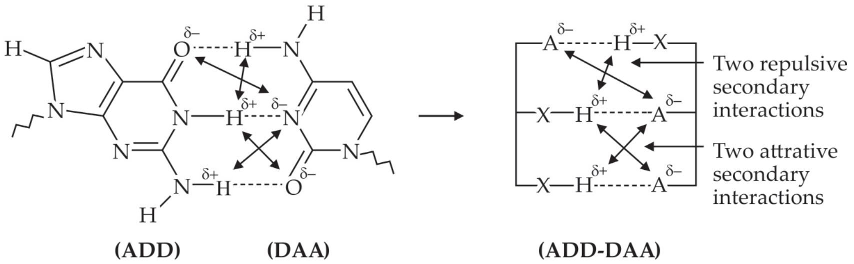

(ADD) **Guanine** **(DAA)** **Cytosine** **(ADD-DAA)**

Fig. 1.3.7.3: Primary and secondary interactions in the Watson–Crick base pair, guanine-cytosine (a representative ADD-DAA system) (see Fig. 2.12.2)

Hydrogen bonding: D—H···A; D—H is the **hydrogen donor** or the **electron acceptor** while A is the **hydrogen acceptor** or **electron donor**.

Halogen bonding: D—X···A; D—X is the **halogen donor** or the **electron acceptor** while A is the **halogen acceptor** or **electron donor**.

D—X may be the halogen molecule (*i.e.* X—X like Br_2, I_2), interhalogen molecule (*e.g.* I—Cl, Br—Cl), organic compound (R—X, Ar—X) or inorganic compound (M—X). The halogen acceptor (A), *i.e.* electron donor is, in general, a good Lewis base (*e.g.* **:**NR_3).

In halogen bonding, the halogen centre (X) acts as the electron acceptor. Thus, the cationic halogen (*i.e.* heavier congener) is the best candidate in halogen bonding. Thus, for CF_3—X, the halogen bond strength in the adduct, F_3C—X···NR_3 increases in the sequence: **X = I > Br > Cl ≫ F.**

In halogen bonding, the noncovalent interactions like **electrostatic, polarisation, dispersion force, charge transfer**, etc. contribute.

$$F_3C\text{—}X^{\delta+}\cdots{}^{\delta-}NR_3,\ X^{\delta-}\text{—}X^{\delta+}\cdots{}^{\delta-}NR_3$$

The **polarisability** and **electropositive character** increase in the sequence, I > Br > Cl > F. Thus, consideration of the electrostatic interaction and dispersive force can explain the order of efficiency of halogen bond: X = I > Br > Cl ≫ F.

Ease of **formation of a polyhalide ion** can be easily explained in terms of the efficiency of halogen bonding. X—X···X^-, where X^- acts as the electron pair donor (*i.e.* Lewis base) as well as the halogen acceptor.

Obviously, this process is most favoured for X = I (*cf.* **polarisability order:** $I_2 > Br_2 > Cl_2 \gg F_2$; **electron donor ability:** $I^- > Br^- > Cl^- > F^-$) and in fact, the observed **stability order** is: $I_3^- > Br_3^- > Cl_3^-$; (F_3^- is not known).

Considering the halogen bonding as the **Lewis acid-base adduct formaiton** (D—X bond acting as the Lewis acid, A acting as the Lewis base), it can be best explained by assuming the donation of nonbonding electron pair of A into the vacant σ*–MO of D—X bond, *i.e.*

Halogen bonding: $n_A(\text{HOMO}) \longrightarrow \sigma^*_{D-X}(\text{LUMO})$;

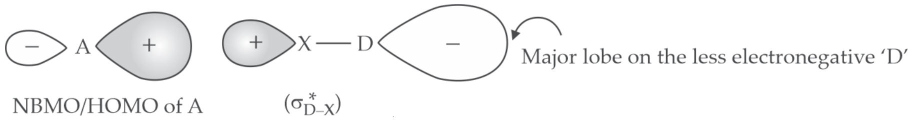

cf. **H-bonding:** D—H···A, $n_A(\text{HOMO}) \longrightarrow \sigma^*_{D-X}(\text{LUMO})$

It is evident that for the **linear D—X···A arrangement, the overlap** between the HOMO of A and LUMO of D—X bond is maximum. It explains the bond angle ($D—\hat{X}\cdots A$) about **180° for the strong halogen bonding**. A similar situation prevails also for the strong H-bonding. The $\sigma_{D—X}$MO is mainly concentrated to the more electronegative centre X while the $\sigma^*_{D—X}$MO is mainly concentrated to the less electronegative D-centre. Obviously, **for the more electronegative X-atom, the electron acceptor orbital** (*i.e.* $\sigma^*_{D—X}$) **becomes more concentrated on D** (*i.e.* $\sigma^*_{D—X}$ of higher energy) and consequently, **the electron acceptance by X through the $\sigma^*_{D—X}$MO becomes less favoured**. In other words, for the halogens, the acceptor $\sigma^*_{D—X}$MO gets concentrated better on X when X is relatively less electronegative. It explains the **efficiency order of halogen bonding**: X = I > Br > Cl > F.

- **3*c*–4*e* bonding model for halogen bonding:** The halogen bonding can be best explained in terms of 3*c*-4*e* bonding as in **H-bonding and closed shell interaction** leading to **secondary bonding** (Sec. 1.3.9). The MO energy diagram for the **3*c*-4*e* halogen bonding** is shown in Fig. 1.3.8.1.

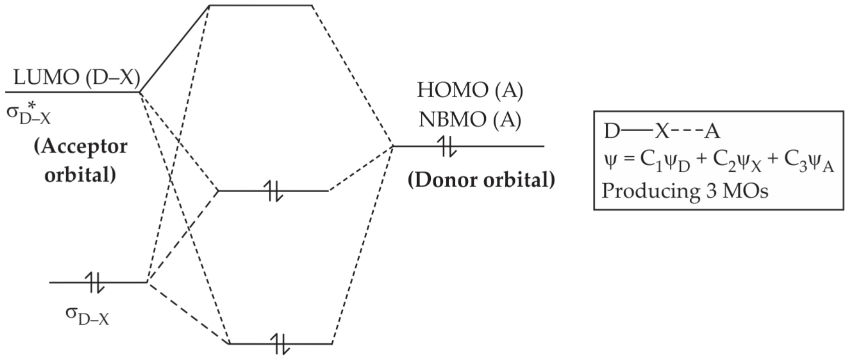

Fig. 1.3.8.1: The MO energy diagram of 3*c*-4*e* halogen bonding (applicable for H-bonding and closed shell interaction) (*cf.* A.K. Das *et al. Coord. Chem. Rev.*, **479**, 215000, 2023)

- **σ-hole theory of halogen bonding** (*Ref.* A.K. Das *et al. Coord. Chem. Rev.*, **479**, 215000, 2023 and the refs. cited therein): Besides the above 3*c*-4*e* covalent bonding model, halogen bonding by the heavier halogens has also been explained by considering the σ-**hole theory** that considers the presence of a σ-**hole of positive potential** on the outermost portion of the halogen atom's surface. It resides along the extension of the D—X covalent bond (say, along the z-axis) for the electronic configuration of halogen (X) as $s^2p_x^2p_y^2p_z^1$. The three nonbonding pairs of electrons of halogen create a belt of negative electrostatic potential around the central part of the halogen atom and consequently, **it produces the positive electrostatic potential in the outermost region of halogen (X)**. In the case of fluorine (*i.e.* D—F bond, X = F), because of the high electron withdrawing inductive effect of fluorine, the bonding electron pair of the D—F bond is shifted towards the outermost surface of F to neutralize the positive electrostatic potential of the σ-hole. This electron withdrawing inductive effect to neutralise the positive electrostatic potential of the σ-hole is determined by the electronegativity order of halogen (X). Thus, the strength of the positive electrostatic potential of the σ-hole runs in the order: I > Br > Cl > F.

Consequently, the strength to accept the electron from A into the σ-hole of the D—X bond in making the halogen bond (D—X···A) increases for the heavier halogens.

In halogen bonding, the **heavier halogen centre** (with the **pronounced relativistic effect** and **more electropositive character**) of the D—X moiety acts as the better electron acceptor by using the vacant σ^*_{D-X} orbital. Obviously, the **electropositive character** (measured by electron deficiency) of the electron acceptor halogen is enhanced when it gets linked with the highly electron withdrawing group (*e.g.* CF_3, F, Cl). This is why, compared to H_3C—X, **F_3C—X is a better candidate for halogen bonding**. It explains why iodine not fluorine of CF_2I—CF_2I acts as the electron acceptor in the self-assembly of this halo-PFC and TMEDA (tetramethyl ethylenediamine) base (Fig. 1.3.8.2).

Self-assembly (a supramolecular architecture) through the halogen bonding has been shown in Fig. 1.3.8.2 for dioxane—Br_2 and $C_2F_4I_2$—TMEDA.

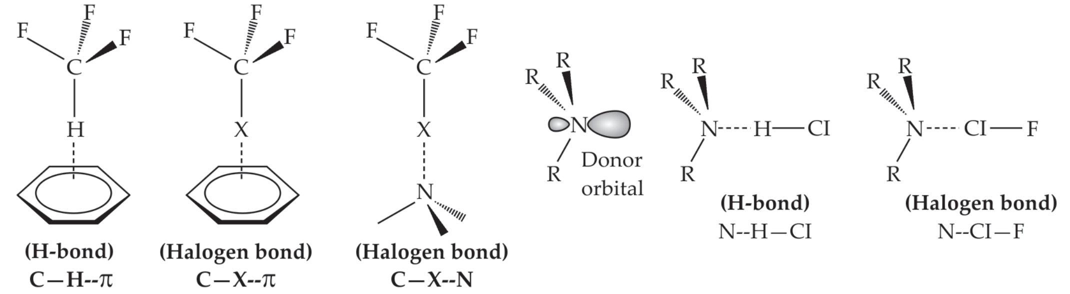

(A) Comparison of hydrogen bonding and halogen bonding

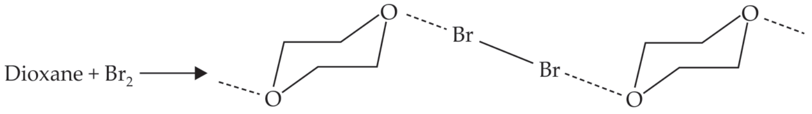

(Self-assembly of dioxane and Br_2 *via* O--Br—Br halogen bonding)

(B) Self-assembly (**1D infinite chain**) between dioxane and Br_2 through halogen bonding

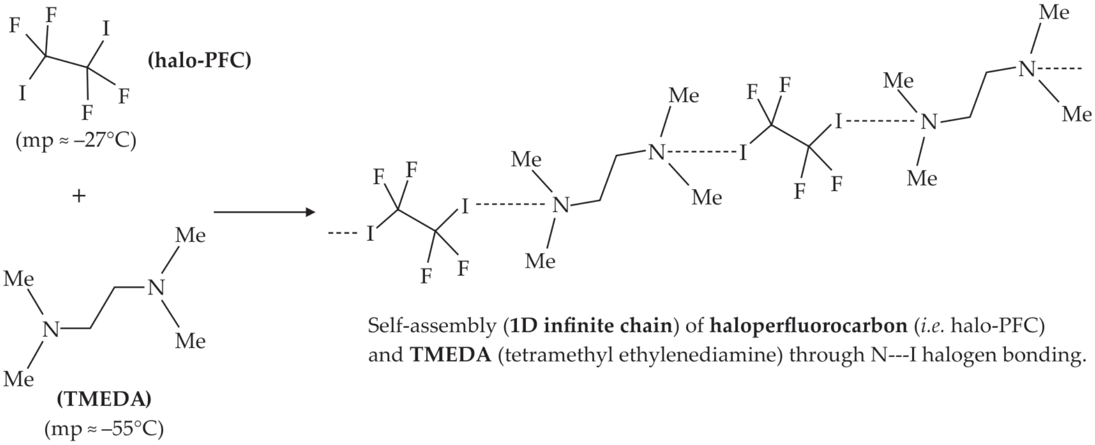

Self-assembly (**1D infinite chain**) of **haloperfluorocarbon** (*i.e.* halo-PFC) and **TMEDA** (tetramethyl ethylenediamine) through N---I halogen bonding.

(C) Self-assembly of diiodotetrafluoroethane and TMEDA (*Ref.* DB Fox *et al, J. Fluorine Chemistry,* **125**, 271, 2004).

Fig. 1.3.8.2: Some examples of halogen bonding and formation of supramolecular architecture (i.e. self-assembly) through halogen bonding (*cf.* Das *et al.*, *Coord. Chem. Rev.*, **479**, 215000, 2023 and the *refs.* cited therein).

Note: Halogen bonding may be also considered as a **closed shell interaction** (leading to secondary bonding) noted for the heavier metals with the electronic configurations d^8 to $d^{10}s^2$ and heavier halogens. The interaction behind ***aurophilicity*** (*i.e.* $Au^I(d^{10})$ ····· $Au^I(d^{10})$ interaction) is also an example of a closed shell interaction.

1.3.9 Closed Shell Interactions—Secondary Bonding, Metallophilicity and Halogen Bonding

The atomic centres with the closed shell electronic configurations can also participate in bonding interaction which is, in general, stronger than the van der Waals interaction but weaker than the covalent interaction. The closed shell interaction is important for the **heavier elements** for which the **relativistic effect** is more important. Due to the pronounced relativistic effect among the heavier congeners, the outermost ***s*- and *p*-orbitals are contracted** (*i.e.* stabilised) and consequently, the bonding electrons placed in such contracted orbitals are stabilised (see Vol. 1 of **Fundamental Concepts of Inorganic Chemistry**). The closed shell interactions occur in metallophilicity like **aurophilicity** (*i.e.* $Au^I(d^{10})$ ······ $Au^I(d^{10})$ interaction), **secondary bonding and halogen bonding**. The relativistic effect on aurophilic interaction has been discussed in detail in Vol. 1 of **Fundamental Concepts of Inorganic Chemistry**.

The halogen bonding has been separately discussed in Sec. 1.3.8. The closed shell or secondary bonding type interaction in X—M···X' (M = multivalent heavy metals like Hg, Tl, Sn, Pb, Bi; X = heavier halogen or chalconide like Cl, Br, S, Se, etc.; X' = O, N, Cl) can be best explained in terms of **3*c*-4*e* bonding**' (*cf*. Fig. 1.3.8.1 for halogen bonding) in which the most important component is the $n(X') \rightarrow \sigma^*_{M-X}$ interaction as in H-bond. Here, X—M is a **normal covalent bond** while M····X′ denotes the **closed shell** or **secondary bonding interaction**.

Aurophilicity (*Ref*. A.K. Das *et al*., *Coord. Chem. Rev*., **479**, 215000, 2023): Here, we shall illustrate the **aurophilic interaction** in short. After maintaining the normal coordination number 2 for the d^{10}-system, Au(I)($5d^{10}6s^0$) shows the additional tendency to introduce the **Au(I) ···· Au(I) interaction** (*ca*. 30–35 kJ mol^{-1}, comparable to H-bonding interaction). Some representative examples of aurophilic interaction are shown in Fig. 1.3.9.1.

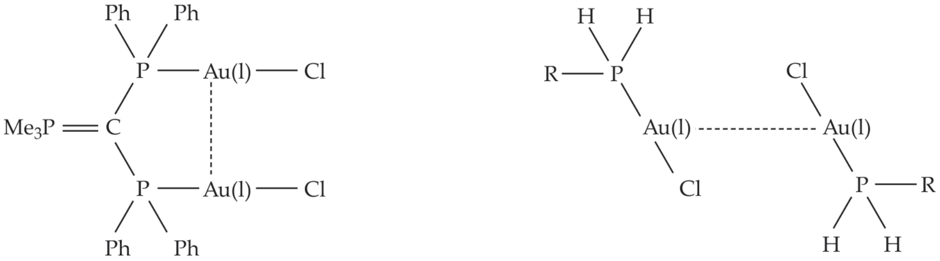

Fig. 1.3.9.1: (a) Intramolecular aurophilic interaction, (b) Intermolecular aurophilic interaction leading to dimerisation (*cf.* ***supramolecular interaction***)

In the **hedgehog cation,** $[C(AuPR_3)_6]^{2+}$ (Fig. 1.3.9.2), the C-centre shows the **hyper-coordination number 6** (*i.e.* each C-centre interacts/binds with the 6 Au centres through the 3*c*-2*e* Au—C—Au bonds). The Au—C—Au interactions are definitely weaker than the normal 2*c*-2*e* bonds. **Overall stability of the cation arises due to these aurophilic interactions**. The hedgehog cation can be simply considered as the combination of

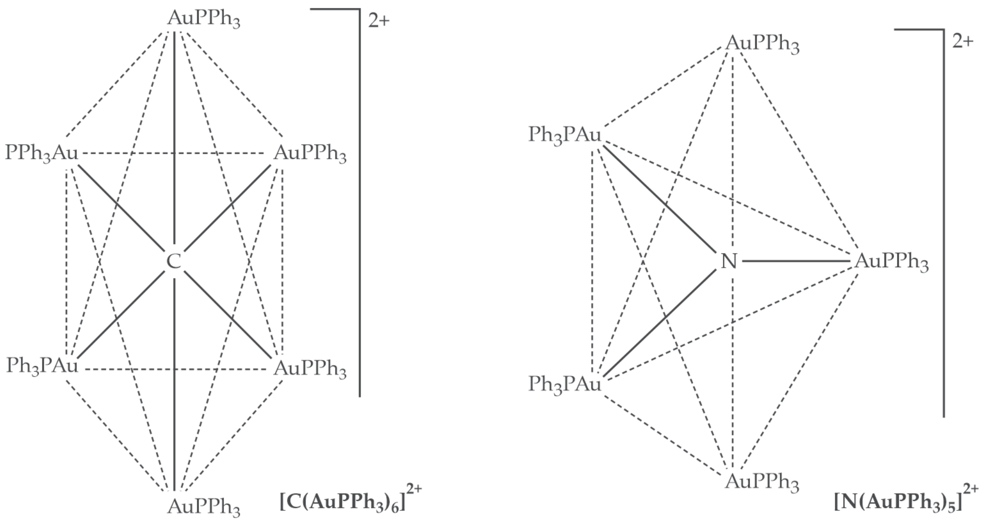

Fig. 1.3.9.2: Aurophilic interaction (shown by dotted lines) in $[C(AuPPh_3)_6]^{2+}$ (*i.e.* hedgehog cation) and $[N(AuPPh_3)_5]^{2+}$

$C^{4-}(2s^22p^6)$ and $6Au(PPh_3)^+$. A similar interaction stabilises the cation, $[N(AuPPh_3)_5]^{2+}$ *i.e.* combination of $N^{3-}(2s^22p^6)$ and $5Au(PPh_3)^+$ in which nitrogen shows the **hypercoordination number 5**. Here the 2 equatorial N—Au bonds (2*c*–2*e*) are formed by the sp^2-hybrid orbitals of N^{3-} and the two axial N—Au bonds (*i.e.* Au—N—Au) are the 3*e*–2*e* bonds (*cf.* in $[C(AuPR_3)_6]^{2+}$, 3 orthogonal 3*c*–2*e* Au—C—Au bonds).

Besides the Au(I)—Au(I) interactions, many other cations called **aurophilic cations** may interact with the Au(I) centre. The examples are: Au(I)—Ag(I), Au(I)—Hg(II), (*cf.* Ag(I) is the lighter congener of Au(I) and Hg(II) is isoelectronic with Au(I)), Au(I)—Tl(I), Au(I)—Pb(II) (*cf.* Tl(I) and Pb(II) are isoelectronic with an inert $6s^2$ pair). In such aurophilic interactions, the aurophilic cations like Ag(I), Hg(II), Tl(I), Pb(II), etc. participitate in the additional interactions with Au(I) after maintaining their own required coordination number, *i.e.* **aurophilicity is not at the cost of inherent coordination number** (Fig. 1.3.9.2).

The additional bonding ability of Au(I) ($5d^{10}6s^0$) can be explaied partly by considering the **relativistic contraction of 6*s*-orbital** and **relativistic expansion of 5*d*-orbital**. It allows the transfer of some electron cloud from the destabilised 5*d*-orbital to the stabilised 6*s*-orbital. **These transferred electrons in the 6*s*-orbital probably participate in the additional bonding interaction**.

1.3.10 Cation-π Interactions

In general, the filled π-orbitals (HOMOs) of the unsaturated organic compounds (*e.g.* olefins, alkynes, aromatics, etc.) may interact with the cations. The representative examples are: $K^+\cdots\pi(C_6H_6)$, $Ag^+\cdots\pi(C_6H_6)$, $X—H\cdots\pi$, $[Fe(\eta^5\text{-}C_5H_5)_2]$, $[Cr(\eta^6\text{-}C_6H_6)_2]$, $[PtCl_3(\eta^2\text{-}C_2H_4)]^-$ (**Zeise's salt anion**), etc. The weak interaction with the nontransition metal ions like alkali and alkaline earth cations is mostly noncovalent but the strong interaction with the transition metal ions is basically covalent (*cf.* $d(M) \leftarrow \pi$ and $d(M) \rightarrow \pi^*$ synergistic interaction) where the vacant metal *d*-orbital receives the electron from the π-BMO (*i.e.* HOMO) of the unsaturated ligand and the filled metal *d*-orbital synergistically donates the electron into the π*-MO of the unsaturated ligand (Fig. 1.3.10.1).

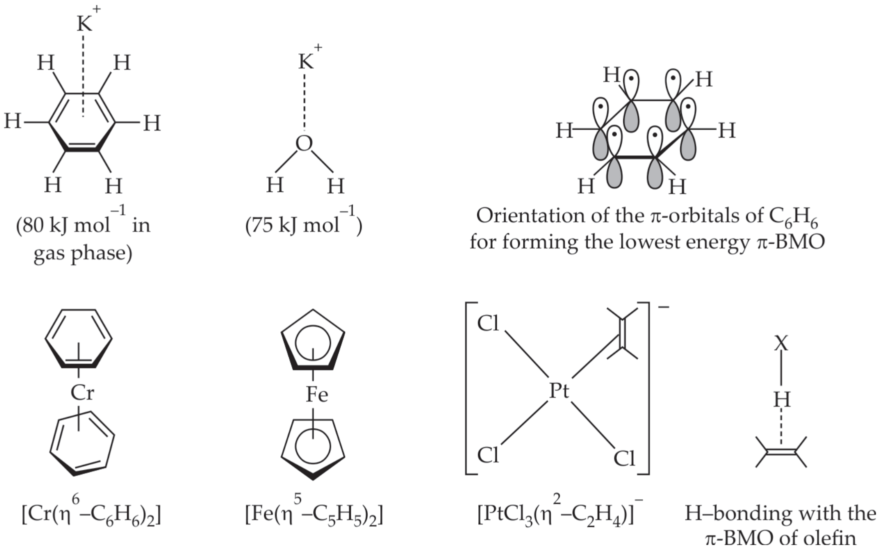

Fig. 1.3.10.1: Some representative examples of cation-π interaction

Note: $K^+\cdots C_6H_6$ *vs.* $K^+\cdots OH_2$ interactions: K^+ is more soluble in water than in C_6H_6 though the **interaction energy with a single water molecule** is comparable to that with a single benzene molecule (*cf.* 80 kJ mol^{-1} *vs.* 75 kJ mol^{-1}). It is due to the fact that **many water molecules** can interact with a single K^+-ion while only **a few** bulkier C_6H_6 molecules can interact with a single K^+-ion.

1.3.11 Anion-π Interaction and Quadrupole Model of Aromatics

An anion being electron rich can electrostatically interact with the **aryl—CH group** (Fig. 1.3.11.1) in which the protonic character is developed on 'H' (*cf.* **χ-value**: sp^2—C > H) and it is expected that **an anion will repel the π-electron cloud of an aryl group**. In fact, it happens so. However, the highly electron deficient unsaturated organic compound having the **low lying (*i.e.* low energy) vacant π*–MO** (acting as the LUMO) can act as the electron acceptor (Fig. 1.3.11.2) from the electron rich moieties including the anions to form the charge transfer complexes. In such charge transfer (CT) complexes, basically the electron deficient species act as the Lewis acids while the anions act as the Lewis bases.

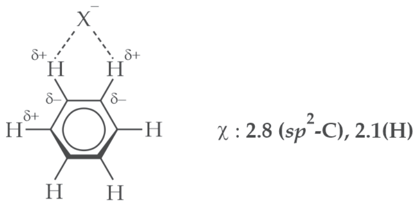

Fig. 1.3.11.1: Illustration of **aryl-CH···anion interaction** (see Fig. 1.3.11.3 to understand the difference from cation-π interaction)

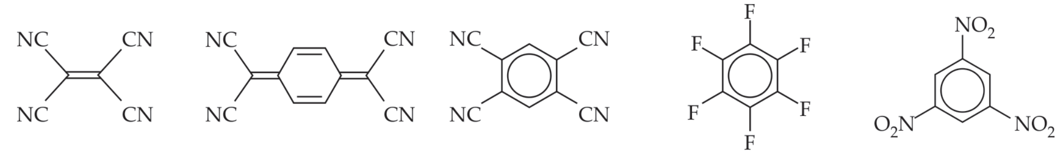

Fig. 1.3.11.2: Some representative examples of electron deficient unsaturated organic compounds with the low-energy vacant π*-MO (*i.e.* low-energy LUMO) **to act as the acceptor in anion-π interaction**

Figure 1.3.11.3 illustrates and compares the cation-π and anion-π interaction. In the anion-π interaction, the electron deficient unsaturated organic compounds act as the electron acceptor.

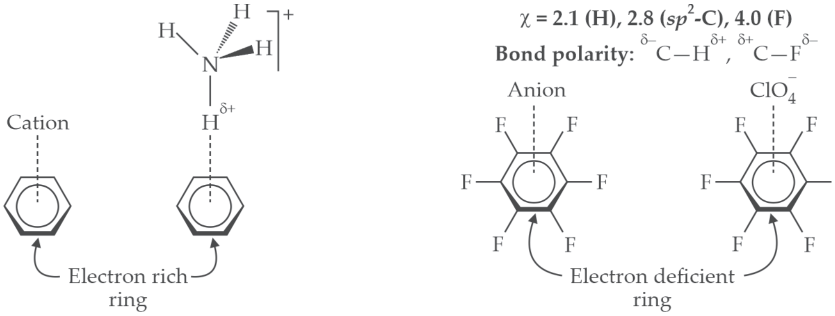

(a) Cation-π interaction **(b) Anion-π (*i.e.*, anion-π*) interaction**

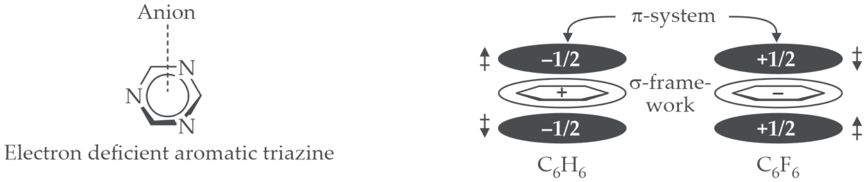

(c) Anion-π (*i.e.*, anion-π*) interaction **(d) π-quadrupoles in benzene and hexafluorobenzene**

Fig. 1.3.11.3: Comparison of **cation**-π (a) and **anion**-π (b, c) interactions; comparison of π-quadrupole of C_6H_6 and C_6F_6(d).

Note: A **quadrupole** having no net charge and no dipole moment consists of two dipoles **oriented antiparallel** as in CO_2 and C_6H_6. The interaction of a quadrupole with an electric field is quantified in terms of its **quadrupole moment**. Similarly, an **octupole** having no net charge and dipole moment consists of 4 dipoles directed towards the 4 corners of a regular tetrahedron as in CX_4.

- **Quadrupole models of C_6H_6 and C_6F_6:** The electron distribution in the delocalised π-bonds of the aromatic rings produces the quadrupole (*i.e.* two dipoles of the same magnitude are aligned in the opposite directions). In C_6H_6, the bond polarity is: $^{\delta-}C—H^{\delta+}$ (χ: sp^2-C > H). The polar σ-bonds lie in the plane of molecule but the charge separated delocalised π-system lies below and above the plane. The polar bonds lead to charge separation as:

negative charges distributed on the both faces (*i.e.* above and below the plane) of π-system balance the positive charges surrounding the edges of the aromatic ring.

Thus, the two dipole moments (working away from the ring) of equal magnitude work in the opposite directions through the centre of C_6H_6 molecule. In C_6F_6, the opposite bond polarity, $^{\delta+}C—F^{\delta-}$ compared to that of the $^{\delta-}C—H^{\delta+}$ bond produces the quadrupole moment opposite to that of C_6H_6 (in terms of direction, not in terms of magnitude). This is schematically shown in Fig. 1.3.11.4.

1.3.12 π–π Interaction: π–π Stacking Interaction

There are different angles of understanding to explain the π-π stacking interaction depending on the conditions.

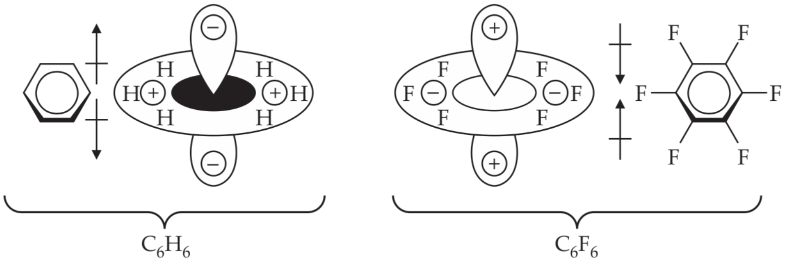

Fig. 1.3.11.4: Quadrupole models of charge separated C_6H_6 and C_6F_6
[Q (quadrupole moment) = –8.48 B for C_6H_6 = +9.5 B for C_6F_6, 1 B (Buckingham) = 3.336×10^{-40} C m^2. 1B = 1 Debye (D) angstrom, 1D = 3.336×10^{-30} C m and 1 Å = 10^{-8} cm = 10^{-10} m]

(A) Balance between the London dispersion force and quadrupole-quadrupole interaction (Hunter-Sanders model): The π–π interaction here considers the interaction between the two aromatic rings. The possible geometries for such interactions are shown in Fig. 1.3.12.1 for (i) a benzene dimer, and (ii) a pair consisting of a **benzene molecule** and a **hexafluorobenzene molecule**. It may be noted that the **sandwich** or **parallel face-to-face** conformation is not noted for a benzene dimer but such a conformation is noted for the C_6H_6–C_6F_6 interacting pair and in **graphite**. In fact, the face-to-face π–π stacking interaction can explain the lubricant properties, slippery feel and electrical conductivity of graphite. However, the **parallel displaced/offset conformation** (attained by offsetting one of the benzene ring) is known to exist for the benzene dimer. Besides this conformation, the **T-shaped** and **edge-to-face conformations** (which are interconvertible through rotation) are also known to exist for the benzene dimers. In fact, the T-shaped and edge-to-face **conformations** are responsible for the characteristic **herringbone packing** in the crystal of benzene and small aromatic hydrocarbons.

The relative stabilities of different conformations of benzene dimer can be explained by considering the **balance between the London dispersion force and quadrupole interactions**. In fact, a benzene molecule may be considered as a **quadrupole** (see Fig. 1.3.11.4), where the σ-framework is positively charged and the delocalised π-system extended below and above the σ-framework bears the equivalent amount of negative charge (*i.e.* **positively charged σ-framework is sandwiched between the negatively charged π-electron cloud**). Thus the two antiparallel dipole moments of equal magnitude are mutually cancelled out (*cf.* the linear CO_2 molecule, O═C═O). The **sandwich conformation** of benzene dimer is stabilised maximum by London dispersion force because in this orientation, the **contact surface area** or the **overlap area for two polarisable π-electron cloud systems is maximum**. But this sandwich conformation is strongly destabilised by the **electrostatic π-π repulsive quadrupole interaction**. It may be noted that in this sandwich conformation, the **attractive electrostatic σ-π quadrupole-quadrupole interaction is relatively less important.**

In the parallel displaced (offset), T-shaped and edge-to-face conformation of **benzene dimer**, the σ-π attractive quadrupole-quadrupole interaction (*i.e. positive quadruple σ-framework of one benzene molecule electrostatically interacting with the negative quadrupole π-framework of another benzene molecule*) stabilises the conformation (Fig. 1.3.12.2). In fact, in these T-shaped and edge-to-face conformations, the favoured σ-π electrostatic attractive

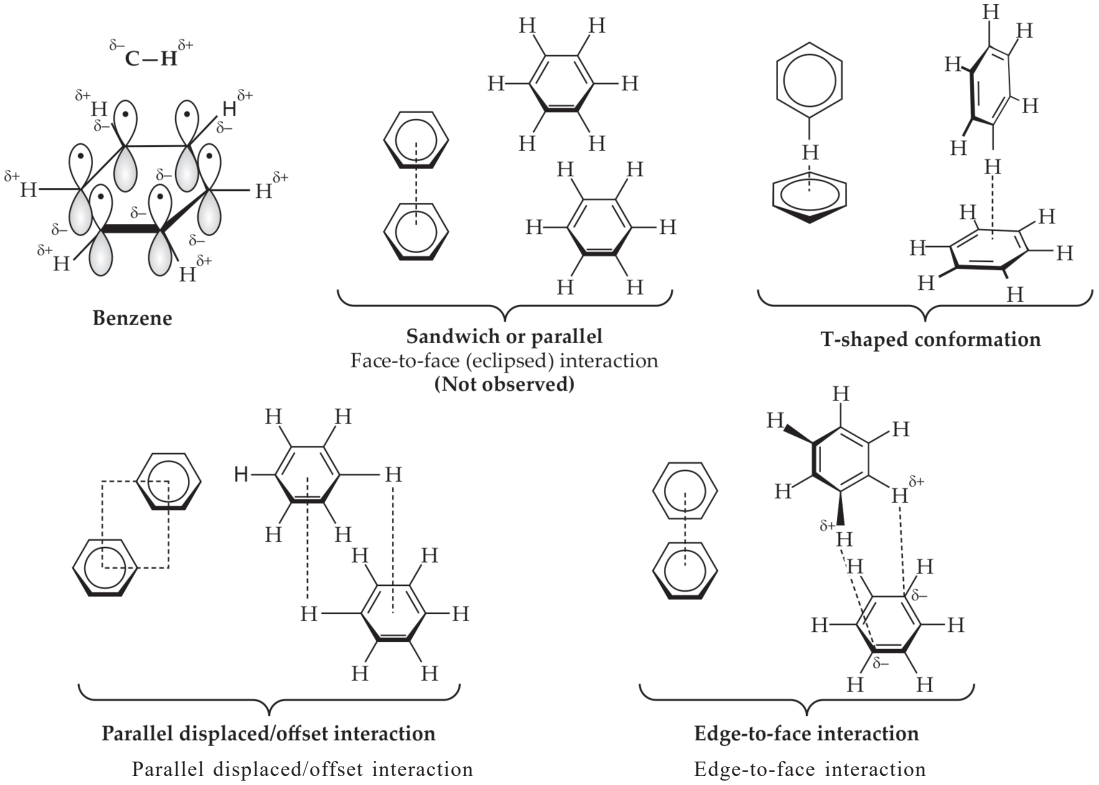

(A) Different conformations for π–π stacking interaction in the **benzene-benzene dimers** (through rotation, the **T-shaped** and **edge-to-face** conformations are mutually interconvertible).

Note: Edge to face interaction in the benzene crystal produces a **herringbone motif** (V-shaped weaving pattern found in many fabrics). It is called so due to the similarity to the bone structure of **herring fish**.

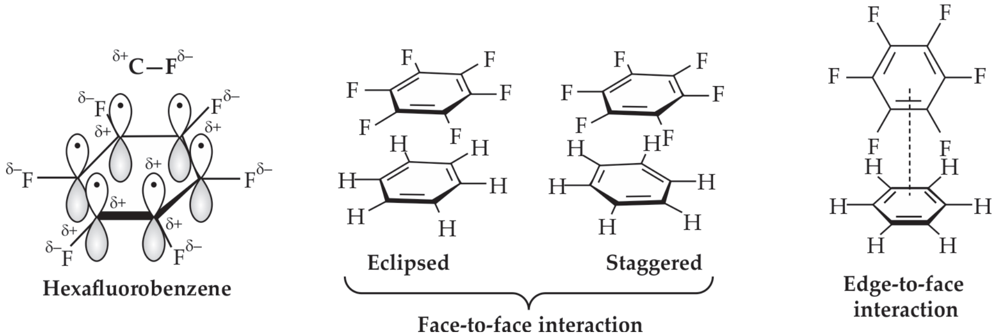

(B) Different conformations for π–π stacking interaction in the **benzene-hexafluorobenzene pair** forming a 1:1 cocrystal (m.p. 297 K > m.p. of C_6H_6 or C_6F_6).

Note: C_6H_6 or C_6F_6 individually fails to show the sandwich, *i.e.* face-to-face, interaction but their 1:1 cocrystals can enjoy the interaction.

Fig. 1.3.12.1: Different geometrical modes of π–π stacking interaction

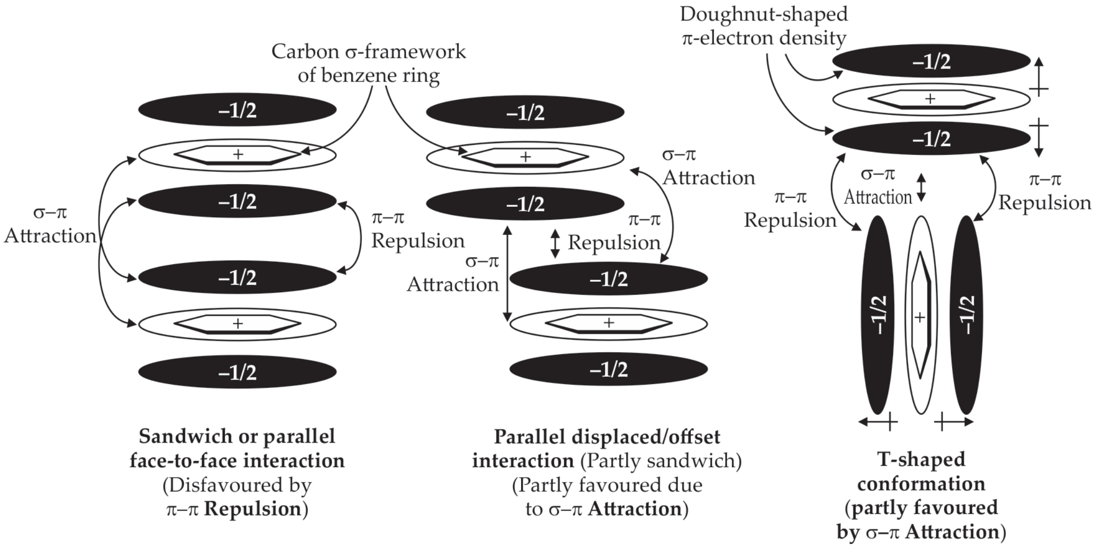

(A) Electrostatic interaction involving the positively charged σ-framework and negatively charged π-electron cloud of benzene in different conformations of the benzene-benzene dimer (*cf.* C.A. Hunter and J.K.M. Sanders, *J. Am. Chem. Soc.*, **112**, 5525, 1990.)

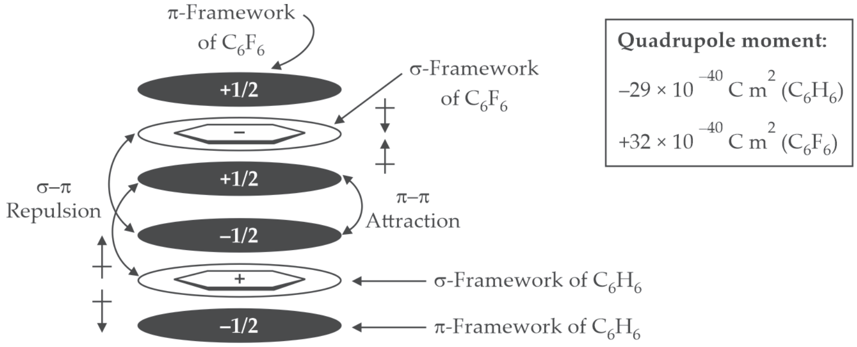

(B) Electrostatic interaction in the **face-to-face conformation** of the benzene-hexafluorobenzene pair (1:1 co-crystal)

Fig. 1.3.12.2: Electrostatic quadrupole/quadrupole ineraction in (A) C_6H_6—C_6H_6 pair and (B) C_6H_6—C_6F_6 pair.

Note: The **face-to-face π–π stacking interaction** is stabilised by the attractive quadrupole-quadrupole σ–π interaction and destabilised by the repulsive π–π interaction in the benzene-benzene dimer.

interaction can compensate the loss of stabilisation energy from the diminished London dispersion force which depends upon the overlap area of the π-ring clouds. The above mentioned balance between the electrostatic quadrupole-quadrupole interaction and London dispersion force to explain the π-π stacking interaction is often described as the **Hunter-Sanders model** (Figs 1.3.12.2 and 1.3.12.3) according to which the **favoured σ-**π attractive quadrupole-quadrupole interaction is the driving force behind the so called π–π stacking interaction.

The quadrupole interaction model for the **$C_6H_6 \cdots C_6H_6$ and $C_6H_6 \cdots C_6F_6$** pairs is simply illustrated in Fig. 1.3.12.3. In C_6H_6, the charge separated $^{\sigma-}$C—H$^{\sigma+}$ σ-bonds lie in the

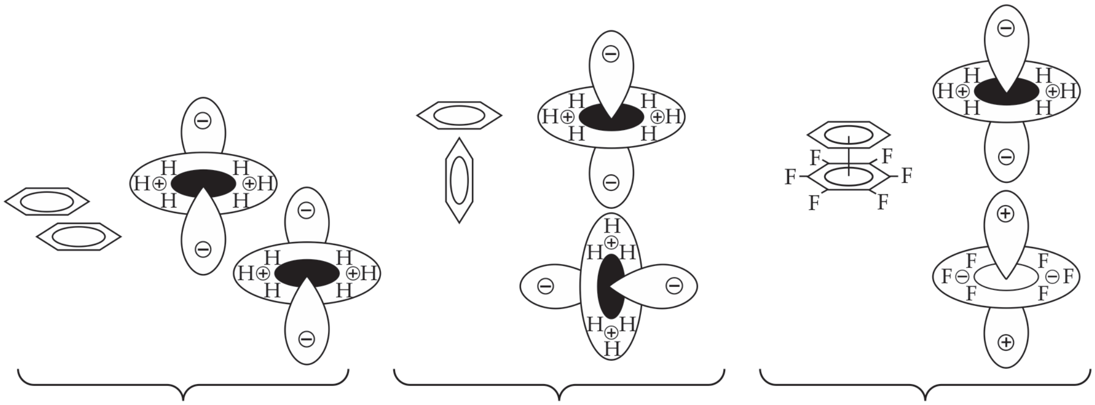

Parallelly displaced **Edge-to-face (T-shaped)** **Face-to-face**

Fig. 1.3.12.3: Simple quadrupole interaction models for $C_6H_6\cdots C_6H_6$ and $C_6H_6\cdots C_6F_6$ pairs

plane of the molecule and the charge separated delocalised π-system lies below and above the plane of the ring. This molecule can be considered as: **the negative charge distributed in the π-system above and below the centre of planar ring balances the positive charges surrounding the edges** (Fig. 1.3.11.4). The opposite bond polarity ($C^{\sigma+}$—$F^{\sigma-}$) in C_6F_6 leads to the charge distribution in an opposite fashion.

T-Shaped and Edge-to-Face Conformation: Representing the π–π Stacking Interaction?

The stability earned in these two conformations can be reasonably explained in terms of **H-bonding interaction** between the slightly electron deficient hydrogen atom (cf. $^{\sigma-}$C—$H^{\sigma+}$ as in aryl—CH bond) of one aromatic ring and the electron rich π-electron cloud of another aromatic ring as in benzene. Thus, this **H-bonding interaction** can be described as: (arene)$\pi_{HOMO} \rightarrow \sigma^*_{C—H}$ (arene) (*cf*. Fig. 1.3.12.1). Such H-bonding interaction is also described as cation-π interaction, in a broader sense. Thus these two conformations should be excluded from the π–π stacking interaction which is relevant to only **face-to-face and parallel-offset conformations**.

(B) **Charge transfer (HOMO → LUMO) interaction:** Besides the electrostatic quadrupole–quadrupole interaction (**Hunter-Sanders model**), the **covalent interaction** (HOMO-LUMO overlap) has been also advocated to explain the **face-to-face π–π stacking interaction** in many cases, specially when one aromatic ring is electron deficient (as in $C_6H_3(NO_2)_3$, C_6F_6) and the other aromatic ring is **electron rich** (as in C_6H_6, $C_6H_3Me_3$). In such cases, HOMO (*i.e.* π-BMO) of the electron rich aromatic ring donates electron into the LUMO (*i.e.* π*-MO) of the electron deficient aromatic ring to produce a **charge transfer (CT) complex, a Lewis acid-base adduct** (see Vol. 2 of Fundamental Concepts of Inorganic Chemistry). The CT-complex may produce a column where the electron donor-acceptor rings are alternately stacked.

(C) **π-type overlap to form a π-band:** In **graphite**, the said HOMO-LUMO interaction is not possible as the interacting components are identical. In graphite, the layer is constituted by **σ-framework** constituted by the sp^2-hybrid orbitals of carbon and the